MOISTURE CONTENT IN DRYING WOOD USING DIRECT SCANNING GAMMA-RAY DENSITOMETRY

John R. Davis

Department of Physics, Monash University
Caulfield East, Victoria 3145, Australia

Jugo Ilic

CSIRO Division of Forest Products
Clayton, Victoria 3168, Australia

and

Peter Wells

Department of Physics, Monash University
Caulfield East, Victoria 3145, Australia

(Received June 1992)

ABSTRACT

The distribution of moisture content in specimens of *Eucalyptus regnans* at various stages of drying from the green state has been measured using a direct scanning gamma-ray densitometer. Densitometry results obtained using 59.5 keV gamma-ray photons were compared with data obtained from matched specimens using a conventional slicing and weighing technique. Preliminary results of a shrinkage distribution analysis are presented for the first time. A detailed discussion of the theoretical and experimental aspects of the scanning densitometry technique is given together with a description of the instrument constructed for this work.

Keywords: Gamma-ray attenuation, wood densitometry, moisture content, shrinkage.

INTRODUCTION

The process of collapse-checking in Australian eucalypts is not well understood. Extensive studies of wood collapse in typical collapse-susceptible species such as *E. regnans* and *E. delegatensis* have clearly established the influence of moisture distribution on collapse development. It is also generally accepted that a lower degree of degrade (check development) occurs when moisture gradients are not severe, particularly during the early stages of drying. Ilic (1983) reported relationships between wood anatomical features and collapse of low density eucalypts and showed that samples with a large proportion of thin-walled earlywood fibers and with large earlywood-latewood density contrasts exhibited a high incidence of internal collapse-checking. The measurement of moisture distribution and density of wood during drying should help to provide a better understanding of the collapse-checking process.

Quantitative measurements of moisture distribution in wood during drying have traditionally involved the invasive and destructive method of weighing thin slices cut from a specimen. The technique can be used to determine shrinkage behavior. However, the destructive nature of the procedure precludes a continuous study of a single specimen.

This paper describes a nondestructive method for measuring moisture content distributions in wood during drying using a scanning gamma-ray densitometer. A similar method was applied by Spolek and Plumb (1981) to determine moisture content in southern pine specimens.

Wood and Fiber Science, 25(2), 1993, pp. 153–162

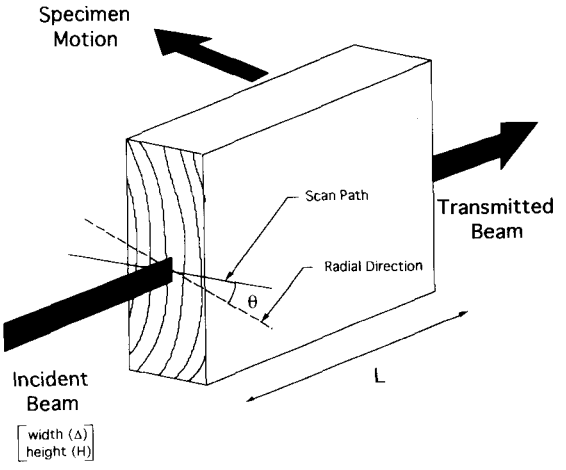

FIG. 1. The scanning densitometer measurement scheme. A collimated gamma-ray photon beam of width Δ and height H is directed through the specimen of thickness L. The scanning path makes an angle θ with the radial direction of the specimen.

PRINCIPLES OF GAMMA-RAY DENSITOMETRY

When a divergence-free beam of gamma-ray or X-ray photons is directed into a material, some photons will be removed from the beam by attenuation processes. The number of photons surviving the passage through the material is related to the quantity of material in the path of the beam. For an homogeneous material of thickness L composed of a single elemental species, the transmission probability for mono-energetic photons is

$$I/I_0 = \exp(-\lambda L) \quad (1)$$

where I_0 is the incident photon intensity, I is the transmitted photon intensity, and λ is the total linear attenuation coefficient of the material. The value of λ depends upon the material bulk density ρ, the atomic number of the material, and the gamma-ray photon energy. The attenuation per unit mass of material in the beam path is given by the mass attenuation coefficient

$$\mu = \lambda/\rho \quad (2)$$

so Eq. (1) may be written as

$$I/I_0 = \exp(-\mu\rho L) \quad (3)$$

It is usual in a scanning densitometry measurement to step-wise translate a specimen of uniform thickness through a collimated gamma-ray beam as shown in Fig. 1. At each step position, i = 1 to N, the beam samples a constant volume of material, and the ratio in Eq. (1) is determined by the mass of attenuating material in that volume. If μ is known, the density of the sampled volume is

$$\rho = (1/\mu L)\ln(I_0/I) \quad (4)$$

When a material consists of a mixture of N elements, the average mass attenuation coefficient can be determined from the mixture rule (Jackson and Hawkes 1981)

$$\mu = \sum_{i=1}^{\mathcal{N}} w_i\mu_i \quad (5)$$

where μ_i is the mass attenuation coefficient of the i^{th} element and w_i is its proportion by mass. The value of ρ in Eq. (4) is then the average density of the material traversed by the gamma-ray beam.

In a scanning densitometry measurement of wood, three gamma-ray photon attenuation processes occur:

1. photoelectric absorption, in which the photon is totally absorbed by the electrons within an atom that, in turn, emits isotropic fluorescent radiation.

2. elastic scattering, often called Rayleigh scattering, in which the incident photon changes direction without loss of energy.

3. inelastic scattering, often called Compton scattering, in which both the direction and energy of the photon may be changed upon interaction with the electrons.

Care must be taken in a densitometry measurement to minimize the detection of scattered photons; otherwise the value of I in Eq. (4) will be increased causing the value of ρ to be underestimated. Elastic scattering tends to be concentrated in the forward direction and its detection can be minimized by using good detector collimation geometry. The contribution from inelastically scattered photons may be removed by the detector electronics pro-

vided that the detector has a sufficiently fine energy resolution capability. For incident photons with the relatively low energy of 59.5 keV used in this work, the energy change on scattering is small and the electronic discrimination of the inelastically scattered photons is not possible. However, at low photon energies, inelastic scattering is nearly isotropic, and good collimation geometry can minimize the detection of inelastically scattered photons.

EQUATIONS FOR MOISTURE CONTENT AND DENSITY

In order to determine the specimen's moisture content, M, and density, ρ, using gamma-ray densitometry, it is necessary to measure the attenuation of the photon beam through the sample in its drying or unequilibrated state. A second, or reference scan, is then performed on the same specimen through the same cross-section with the specimen in a known equilibrium moisture state. Throughout this experiment, the equilibrated state used was the oven-dried condition. A set of scan data is referred to as a profile.

The purpose of this section is to present the equations that allow the experimental determination of the unequilibrated moisture content of the specimen and the unequilibrated specimen density at each measuring position of a densitometry scan. The full derivations of the relevant expressions are contained in Appendix A, and only the necessary equations are reproduced here.

To distinguish between the states of the specimen, the symbols are used with a subscript d to identify the oven-dried state. The subscript w is used for those measurements and parameters that pertain specifically to water. In determining the value of the moisture content and density at each step, or within each sampled volume, of a scanning densitometry measurement, it is assumed that the specimen consists of two attenuating components: wood and total water (free and bound). These two components are distributed throughout the specimen thickness, L, within the sampled volume, V.

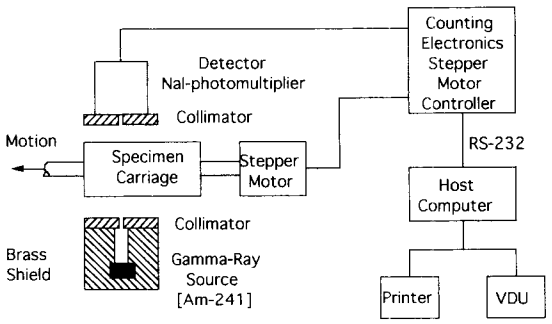

FIG. 2. The schematic layout of the scanning densitometer.

From Eqs. (A9) the moisture content at each step in the unequilibrated specimen scan may be expressed as

$$M = \frac{\mu}{\mu_w}\left\{\frac{VL_d \ln(I_0/I)}{V_d L \ln(I_0/I_d)} - 1\right\} \tag{6}$$

The average density of material ρ in the unequilibrated sample volume is, from Eq. (A11)

$$\rho = \frac{V_d(1 + M)\ln(I_0/I_d)}{V\mu L_d} \tag{7}$$

In the oven-dried case, the density may be obtained directly from Eq. (A12) as

$$\rho_d = \frac{\ln(I_0/I_d)}{\mu_d L_d} \tag{8}$$

These equations allow the values of the moisture content, M, and the density, ρ, to be calculated at each step of a densitometry scan provided the volume ratio (V/V_d) can be determined. To obtain this ratio, it is necessary to devise a strategy to correct for the dimensional change of the specimen on oven-drying from the unequilibrated state. The correction method, described in Appendix B, also takes into account the anisotropic nature of the specimen and allows for situations where the scan path of the beam is not radial (Fig. 1).

DESCRIPTION OF THE DENSITOMETER

A schematic diagram of the densitometer constructed for this work is shown in Fig. 2. This instrument is similar to densitometer systems reported elsewhere (Cown and Clement

TABLE 1. *Drying time in a 12% EMC environmental chamber (35 C and 85% RH) for matched-pair specimens prior to densitometer (A) and slicing and weighing (B) measurements.*

Matched pair specimens		Drying time at measurement (days)
(1A, 1B)	(6A, 6B)	Zero (Green)
(2A, 2B)	(7A, 7B)	3
(3A, 3B)	(8A, 8B)	10
(4A, 4B)	(9A, 9B)	22
(5A, 5B)	(10A, 10B)	53

1983; Laufenberg 1986; Winistorfer et al. 1986). The radiation source is a 200 mCi (7.14 GBq), 5-mm-diameter bead of Am-241 (59.5 keV) sealed in a stainless steel cylinder (Amersham International AMC.26) and contained in a radiation shield holder made of brass. Gamma-ray photons are detected using a sodium-iodide (thallium) scintillation crystal-photomultiplier detector (Canberra Nuclear Products Group Model 1701). A brass sleeve of 5-mm wall thickness encloses the detector and shields it against scattered radiation from the specimen and other low energy radiation.

Pairs of matched brass collimators, each 10 mm thick in the beam direction, having rectangular slits 4 mm high and widths of 0.25 mm, 0.5 mm and 1 mm, may be attached to the source holder and the detector shield. The source holder is mounted on a horizontal micrometer stage that permits accurate alignment of the collimating slits. The distance between the source and detector collimators can be varied from 60 mm to 150 mm to accommodate a range of specimen thicknesses.

The specimen to be scanned is translated step-wise through the collimated gamma-ray beam on a stepper-motor driven stage. Limit switches at the extremes of the stage movement provide references for specimen positioning. The stage assembly can accommodate specimens up to 300 mm in length.

Data acquisition, system control, interface electronics, and high and low voltage regulated power supplies are housed in a single module. This module provides a single RS232 link to a host PC-AT microcomputer. An MC6803 microprocessor in the module serves as the hub of the system.

Voltage pulses generated by the photomultiplier, upon detection of gamma-ray photons in the scintillator crystal, are shaped and passed to a pulse-height analyzer (PHA) unit that selects pulses produced by the 59.5 keV photons. These pulses are presented to a counter-timer scaler. The system dead-time is about 1 μsec. The counter-timer scaler may be operated in either a preset-time or preset-count acquisition mode. In the preset-time mode, the scaler accumulates pulses for predetermined time intervals selectable from 0.1 sec to 1,000 sec. For the preset-count mode, the time taken to reach a preset value, selectable from 1,000 counts to 1,000,000 counts, is recorded as an integral number of 10 μsec timing intervals. In the preset-count mode all recorded scan data will have the same statistical uncertainty.

EXPERIMENTAL DETAILS

Specimen preparation

Five pairs of matched contiguous specimens were cut from each of two green back-sawn boards of mountain ash (*E. regnans*). The specimen dimensions were typically 95 mm by 45 mm in cross-section and 100 mm along the grain direction. All specimens were wrapped in thin plastic foil and stored at 4 C before drying. The specimens were dried for various periods (Table 1) in a 12% equilibrium moisture content (EMC) chamber.

Matched-pair specimens were labelled as 1A, 1B to 5A, 5B for one board and 6A, 6B to 10A, 10B for the other board. The A specimens were scanned in the densitometer. Independent weighing and volume measurements were made on sliced samples extracted from the B specimens. Measurements were made at various times over a period of 53 days. Densitometry and slicing measurements were carried out simultaneously on the unequilibrated specimens.

Densitometer measurements

Prior to scanning, the specimen mass, its dimensions and bulk density, and the angle

between the scan profile path and the specimen radial direction (Fig. 1) were measured. Specimens were scanned while wrapped in thin plastic foil to minimize moisture change during scanning.

Collimators were selected to give a nominal beam cross-section of 4 mm high by 0.5 mm wide with a source-to-detector collimator separation of 110 mm. The gamma-ray count rate without a specimen was about 600 counts/sec and the stepping interval was 0.5 mm. Counting was performed in the preset-time mode using a preset value of 20 sec. After each scan the specimen mass and dimensions were remeasured with no observable changes apparent.

The higher moisture content specimens were air-dried in the laboratory before oven-drying to minimize the formation of additional collapse degrade. Each specimen was oven-dried at 102 C until its mass became constant. The bulk density and moisture content of each specimen were determined at the time of scanning. A densitometry scan of each oven-dried specimen, again wrapped in plastic foil, was carried out along the initial scan path.

Slicing and weighing measurements

A cylindrical core sample of 25 mm diameter was extracted from each B specimen and sliced into 2-mm-thick discs as shown in Fig. 3. Each disc was weighed and its volume measured using the mercury displacement method (Chafe 1985).

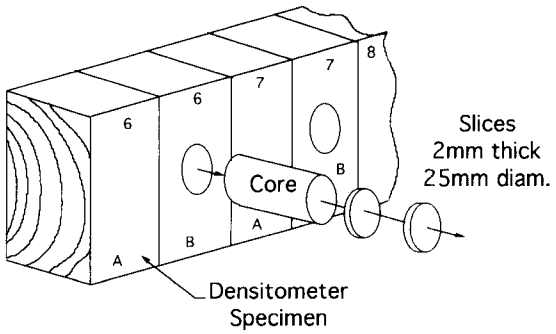

FIG. 3. Matched-pair specimens in a sawn board. Each A specimen was scanned in the densitometer. Measurements were also made on 2-mm-thick discs sliced from a 25-mm-diameter core extracted from each B specimen.

EXPERIMENTAL RESULTS

Densitometer measurements

Values of the mass attenuation coefficient of dry wood, μ_d, were obtained from the oven-dry scan data for each specimen using Eq. (A16). The value of μ_d averaged over all ten specimens was found to be 0.0189 ± 0.0002 $m^2\ kg^{-1}$.

The experimentally determined value of the mass attenuation coefficient of water, μ_w, at 59.5 keV was found to be 0.0200 ± 0.0002 m^2kg^{-1}. This result is in reasonable agreement with the value of 0.02048 $m^2\ kg^{-1}$ deduced from the most recently tabulated theoretical photon-atom cross-section data (Cullen et al. 1989). The lower experimental value may be attributed to a small contribution from either multiple scattering or the unavoidable inelastic forward scattering.

Scan data for the oven-dry state were corrected for shrinkage as described in Appendix B. In this procedure, a segmented region approach was adopted to allow for non-uniform shrinkage during drying. Within each segmented region, the shrinkage was assumed to be uniform. The number of data values (or increment steps) in corresponding segments of the unequilibrated and oven-dried states were denoted as n ($n \leq N$) and n_d ($n_d \leq N_d$), respectively. The expression for the volume ratio V/V_d derived from Eq. (B14) then becomes

$$\frac{V}{V_d} = \left[\frac{Ln}{L_d n_d}\right](1 + \gamma) \qquad (9)$$

The quantity γ, defined in Appendix B, takes into account the dimensional changes in the tangential and radial directions and allows for situations where the scanning path of the gamma-ray beam is not parallel to the radial direction (Fig. 1). In the evaluation of γ, a value of 2 (Kingston and Risdon 1961) was used for the tangential-to-radial shrinkage ratio of *E. regnans*.

The moisture content M and density ρ at

TABLE 2. *Summary of the average density and moisture content results obtained from scan data (sc) and the whole specimen (s) for each of the densitometer (A) specimens.*

Specimen	Average density (kg m $^{-3}$)				Average moisture content (percent)	
	ρ_s	ρ_{sc}	$\rho'_{s,d}$	$\rho'_{sc,d}$	M_s	M_{sc}
1A	961	1,016	481	465	149	153
2A	831	894	491	459	94	95
3A	642	681	510	510	38	39
4A	588	593	545	552	14	12
5A	536	551	537	529	9	7
6A	1,014	1,032	523	526	149	145
7A	887	936	519	518	104	101
8A	650	696	526	547	32	34
9A	577	592	531	572	13	10
10A	564	583	537	572	9	8

each step in a scan of N total steps are obtained from Eqs. (6) and (7) as

$$M = \left[\frac{\mu n}{\mu_w n_d}\right](1 + \gamma)\left[\frac{\ln(I_0/I)}{\ln(I_0/I_d)} - 1\right] \quad (10)$$

$$\rho = \frac{n(1 + M)\ln(I_0/I_d)}{n_d \mu_d L(1 + \gamma)} \quad (11)$$

The experimentally determined values of μ_d and μ_w quoted previously were used in the above calculations. Profiles of moisture content and unequilibrated density in each specimen were obtained using Eqs. (10) and (11), respectively. Average values of density and moisture content obtained from the densitometer and slicing measurements are presented in Tables 2 and 3. For the densitometer specimens, there is good agreement between the values for the whole specimen (s) and the average scan data (sc).

TABLE 3. *Average density and moisture content results obtained from the unequilibrated sliced (B) samples.*

Specimen	Average density (kg m $^{-3}$)	Moisture content (percent)	
		M_{core}	M_{discs}
1B	995	150	154
2B	884	88	90
3B	677	40	41
4B	593	16	16
5B	557	11	11
6B	1,025	145	145
7B	925	97	98
8B	696	36	36
9B	594	14	14
10B	575	10	10

The differences in the moisture content values for the slicing results in Table 3 are a consequence of the definition of moisture content. The moisture content of the cylindrical core, derived from data for $\mathcal{N}$ individual discs, is given by

$$M_{core} = \left[\frac{\sum_{i=1}^{\mathcal{N}} m_i - \sum_{i=1}^{\mathcal{N}} m_{d,i}}{\sum_{i=1}^{\mathcal{N}} m_{d,i}}\right] \quad (12)$$

where m and m_d are the masses of a disc in the unequilibrated and oven-dry states, respectively. The average moisture content of $\mathcal{N}$ individual discs is found from

$$M_{discs} = \frac{1}{\mathcal{N}} \sum_{i=1}^{\mathcal{N}} \left[\frac{m_i - m_{d,i}}{m_{d,i}}\right] \quad (13)$$

In general, $M_{core} \leq M_{discs}$ and the results in Table 3 are consistently in accord with this relationship. This relationship does not hold for the moisture content data in Table 2 since the results for the whole specimen moisture content M_s and average scan moisture content M_{sc} were not derived from the same volume of material.

Typical density and moisture content profiles for the matched pair specimens 2A and 2B, are presented in Fig. 4a and 4b. The oven-dried densitometer density profiles were corrected for dimensional change to allow registration with the unequilibrated profiles.

Estimate of shrinkage distribution from densitometer scan data

The results reported in this paper represent density and moisture content distributions in different specimens at different stages of drying from the green state. The shrinkage distribution profile in specimen 2A after oven-drying from an average moisture content of 95% is shown in Fig. 5. Shrinkage data were obtained by a segmented comparison of corresponding

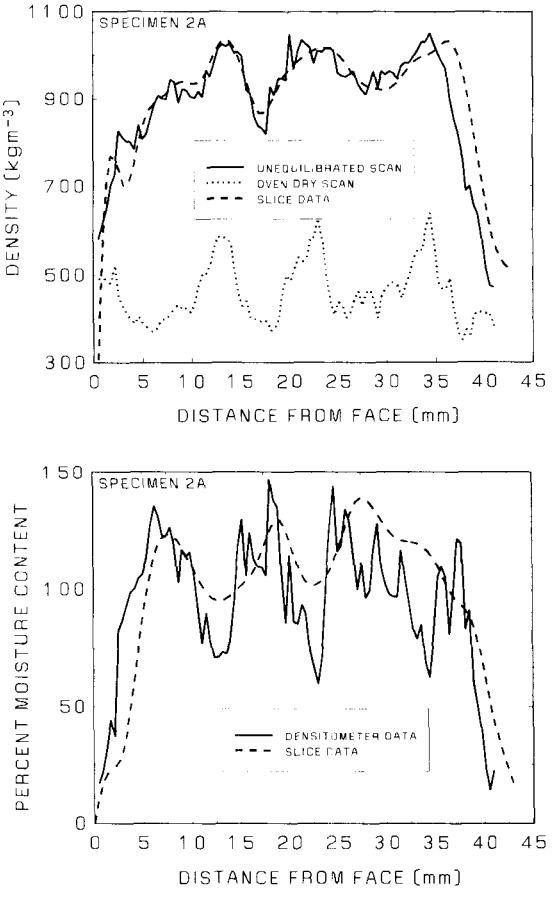

FIG. 4. (a) Density and (b) moisture content profile data for matched-pair specimens 2A and 2B. The curves are spline fits to the data.

length segments in the unequilibrated and oven-dry density profiles. The shrinkage values δ were calculated using the expression

$$\delta = \frac{l - l_d}{l} \qquad (14)$$

where l and l_d are the lengths of corresponding regions in the unequilibrated and oven-dry density profiles, respectively.

DISCUSSION

Moisture content and density distributions

Given the expected smoothing effect on the density and moisture content profile data inherent in the slicing method, and the varying

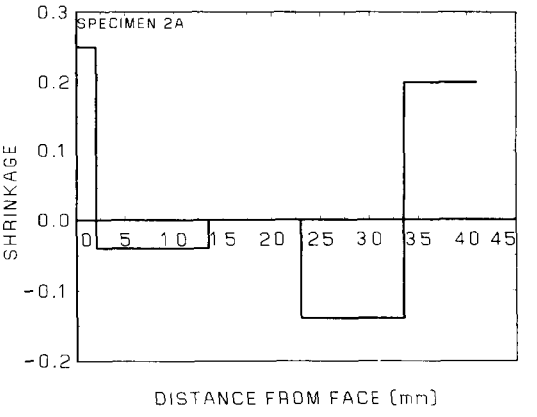

FIG. 5. The shrinkage distribution profile for specimen 2A deduced from densitometer scan data. Positive and negative values are indicative of compressive and tensile strains, respectively.

grain direction over the length of the matched pairs of specimens, the densitometry data agree extremely well with the independently measured slicing data. Absolute uncertainties in the densitometry moisture content values ranged from ±3% at 150% to ±2% at 10%. The uncertainties in density values ranged from ±20 kg m^{-3} to ±6 kg m^{-3} at high density-high moisture content (1,000 kg m^{-3}) and oven-dry states (550 kg m^{-3}), respectively.

The principal factors contributing to uncertainties in the densitometer results arise from:

1. the experimental determination of μ_d and μ_w. It is usually expected that these values will be underestimated because of the unavoidable detection of scattered photons. It should be possible to estimate the fraction of the incident photon flux scattered into the detector collimator aperture using Monte Carlo methods. The simulation of gamma-ray photon scattering from wood is the subject of a current investigation.

2. the measurement of the specimen thickness L. Calculations of density and moisture content assume that the thickness of the specimen in the gamma-ray beam direction is constant at all steps in a scan. Hence, it is important that specimens are accurately machined. Given that this condition is achieved, L may be measured to better than 1%.

3. statistical fluctuations in I_0, I and I_d. The incident (unattenuated) count I_0 can be measured to high statistical precision. Uncertainties in I and I_d are determined by the preset conditions for data collection.

4. the procedure used to correct the oven-dry scan data for dimensional change. The segmented approach adopted for this work is probably satisfactory for stepping increments of 0.5 mm.

In any scanning densitometry measurement, the raw attenuation data profile represents a convolution of the distribution of attenuating mass within the specimen and the resolution function of the instrument. Factors that contribute to the instrument resolution function include the beam geometry within the specimen and the collimation geometry, particularly at the detector. In practice, collimated beams are not parallel and do not have a uniform cross-sectional flux distribution. The model used in this work does not account for these factors. However, for the rather coarse resolution employed in this study and, given that grain direction variation of at least 0.5 mm can occur in a thick specimen, the ideal parallel beam assumption is reasonable.

Shrinkage distribution

The shrinkage profile data of Fig. 5 are consistent with the drying strains that occur after wood dries from the green state to the oven-dry state. The strain in specimen 2A is compressive near the surface and becomes tensile towards the core.

These preliminary results demonstrate that the scanning densitometry technique provides a measure of the spatial distribution of shrinkage within a specimen during drying. Future work in this area will involve the use of two-dimensional X-ray tomography data of green state specimens to study the shrinkage and strain distributions within specimens during drying to an equilibrated state. This information should help to determine optimal drying schedules for collapse-prone eucalypt species.

CONCLUSIONS

Direct scanning gamma-ray densitometry can yield accurate and precise quantitative information about bulk density and moisture content distributions in wood during drying. The technique has the potential to provide information about shrinkage and strain distributions in wood, particularly eucalypt species, during drying.

ACKNOWLEDGMENTS

The densitometer was constructed by Nino Benci and Ross Harrop from the Department of Physics at Monash University. Rhys Davies from the Department of Physics produced the illustrations. Ms. Margaret Walker from CSIRO Division Forest Products carried out the slicing and weighing measurements.

REFERENCES

CHAFE, S. C. 1985. The distribution and interrelationship of collapse, volumetric shrinkage, moisture content, and density in trees of *Eucalyptus regnans* F. Muell. Wood Sci. Technol. 19:329–345.

COWN, D. J., AND B. G. CLEMENT. 1983. A wood densitometer using direct scanning with X-rays. Wood Sci. Technol. 17:91–99.

CULLEN, D. E., M. H. CHEN, J. H. HUBBELL, S. T. PERKINS, E. F. PLECHATY, J. A. RATHKOPF, AND J. H. SCOFIELD. 1989. Tables and graphs of photon-interaction cross-sections from 10eV to 100GeV derived from the LLNL evaluated Photon Data Library (EPDL), UCRL-50400, Vol. 6.4.

ILIC, J. 1983. The development of rapid automatic systems for measurement of wood anatomical characteristics and their application to wood properties. M.App.Sci. thesis (unpublished), Chisholm Institute of Technology, Caulfield East, Victoria, Australia.

JACKSON, D. F., AND D. J. HAWKES. 1981. X-ray attenuation coefficients of elements and mixtures. Physics Reports 70:169–233.

KINGSTON, R. S. T., AND C. J. E. RISDON. 1961. Shrinkage and density of Australian and other South-West Pacific woods. CSIRO Div. For. Prods., Tech. Paper No. 13, Melbourne, Australia.

LAUFENBERG, T. L. 1986. Using gamma radiation to measure density gradients in reconstituted wood products. Forest Prod. J. 36:59–62.

SPOLEK, G. A., AND O. A. PLUMB. 1981. Capillary pressure in softwoods. Wood Sci. Technol. 15:189–199.

WINISTORFER, P. M., W. C. DAVIS, AND W. W. MOSCHLER. 1986. A direct scanning densitometer to measure wood composite products. Forest Prod. J. 36:82–86.

APPENDIX A

In this Appendix the same convention is used regarding the subscripts as in the body of the paper. In order to derive general expressions for equilibrated measurements and parameters (and not just for the special case of oven-dried), a prime is used.

Using Eqs. (2) and (4), the product λL for corresponding sampled volumes in the unequilibrated and equilibrated states of a scanned specimen is given by

$$\lambda L = [\mu_d \rho + \mu_w \rho_w]L \tag{A1}$$

$$\lambda' L' = [\mu_d \rho' + \mu_w \rho'_w]L' \tag{A2}$$

Here, μ_d is the mass attenuation coefficient of dry wood, μ_w is the mass attenuation coefficient of water, L is the specimen thickness in the beam direction, ρ and ρ' are the partial densities of wood in the unequilibrated and equilibrated states, and ρ_w and ρ'_w are the partial densities of total water in the aforementioned states, respectively. Partial density is defined as the ratio of the mass of component material (wood or total water) to the volume sampled by the collimated gamma-ray beam.

The moisture content M in a sampled volume at each step is the ratio of the total water mass m_w to the mass of oven-dry wood m_d. For the unequilibrated and equilibrated states, the moisture contents are

$$M = m_w/m_d \tag{A3}$$

$$M' = m'_w/m_d \tag{A4}$$

or in terms of partial densities

$$M = (\rho_w V)/(\rho_d V_d) \tag{A5}$$

$$M' = (\rho'_w V')/(\rho_d V_d) \tag{A6}$$

where V and V′ are the unequilibrated and equilibrated sampled volumes, V_d is the corresponding oven-dry volume, and ρ_d is the dry wood density for that volume. Using Eqs. (3), (A5) and (A6), Eqs. (A1) and (A2) become

$$\lambda L = [\mu_d \rho_d (V_d/V) + \mu_w \rho_d M(V_d/V)]L = \\ = \ln(I_0/I) \tag{A7}$$

$$\lambda' L' = [\mu_d \rho_d (V_d/V) + \mu_w \rho_d M'(V_d/V)]L' = \\ = \ln(I_0/I') \tag{A8}$$

where I and I′ are the measured transmission intensities in the two scans.

From Eqs. (A7) and (A8), the moisture content at each step in the unequilibrated specimen scan may be expressed as

$$M = ABC + D \tag{A9}$$

where

$$A = (\mu_d/\mu_w)$$

$$B = 1 + [(\mu_w VL'M')/(\mu_d V'L)]$$

$$C = \left[\frac{(VL'/V'L)[1 + (\mu_w M'/\mu_d)]\ln(I_0/I)}{B \ln(I_0/I')}\right] - 1$$

$$D = (M'VL'/V'L)$$

The average bulk density of material, ρ, in the unequilibrated sampled volume is the sum of the partial densities

$$\rho = \rho_d + \rho_w = \rho_d(V_d/V)(1 + M) \tag{A10}$$

and using Eq. (A8), Eq. (A10) becomes

$$\rho = \frac{(V'/V)(1 + M)\ln(I_0/I')}{\mu_d L'[1 + (\mu_w M'/\mu_d)]} \tag{A11}$$

The average bulk density in the equilibrated sampled volume is

$$\rho' = \frac{(1 + M')\ln(I_0/I')}{\mu_d L'[1 + (\mu_w M'/\mu_d)]} \tag{A12}$$

The mass attenuation coefficient of dry wood μ_d may be determined using the equilibrated specimen scan data. Rearranging Eq. (17), we have for the i^{th} step in a scan of N′ steps

$$(\mu_d + \mu_w M')L'\rho'_i = (1 + M')\ln(I_0/I'_i) \tag{A13}$$

where μ_d, M′ and L′ are assumed constant for the entire specimen. Summing over all N′ scan steps and averaging yields

$$(\mu_d + \mu_w M')L'\left[\frac{1}{N'}\sum_{i=1}^{N'} \rho'\right] = \\ = (1 + M')\left[\frac{1}{N'}\sum_{i=1}^{N'} \ln(I_0/I')\right] \tag{A14}$$

Assuming, for an equilibrated specimen, the average density of the densitometry scan is equal to the bulk denisty ρ'_s of the entire specimen, then

$$\frac{1}{N'}\sum_{i=1}^{N'} \rho'_i = \rho'_s \tag{A15}$$

and from Eq. (A14), the mass attenuation coefficient of dry wood is given by

$$\mu_d = \left\{\left[\frac{(1 + M')}{L'\rho'_s N'}\right]\sum_{i=1}^{N'} \ln(I_0/I'_i)\right\} - \mu_w M' \tag{A16}$$

Once values of μ_w and μ_d are known, the values of M, ρ and ρ' in Eqs. (A9), (A11), and (A12) can be calculated at each step of a densitometry scan provided the volume ratio (V/V′) can be determined (see Appendix B). For the experiment described in this paper, as mentioned previously, all equilibrated specimens are in the oven-dried condition, and the appropriate equations were obtained by setting all the primed symbols to their oven-dried equivalents, and noting that $M_d = 0$.

APPENDIX B

To determine the moisture content and bulk density in the unequilibrated specimens, the equilibrated scan data

must be subtracted from unequilibrated data. The radial and tangential dimensions of the specimen in the equilibrated state will be less than those in the unequilibrated state. Consequently, the equilibrated state data must be transformed or stretched to register with the unequilibrated state data prior to subtraction. The transformation strategy used in this work is described below.

Using the same notation as in the main text and Appendix A, let the number of data values or steps in the unequilibrated and equilibrated scans be N and N′, respectively, with $N \geq N'$. Denote by Δ, the scan step length (width of the gamma-ray beam) for both scan measurements. The equilibrated data file is then stretched so that these data are now associated with step increments of width Δ', with $\Delta' \geq \Delta$. Since the scan data sets now have the same overall length, then

$$N\Delta = N'\Delta' \tag{B1}$$

This stretched data set is then mapped into a set of N values, each associated with an increment Δ prior to subtraction from the unequilibrated data set.

Define $\{E_n : 1 \leq n \leq N'\}$ to be the set of stretched raw equilibrated data and the set $\{E^t_m : 1 \leq m \leq N\}$ to be the transformed equilibrated data set. To map the set $\{E_n\}$ into $\{E^t_m\}$, it is necessary to know where the m^{th} increment in $\{E^t_m\}$ is located in $\{E_n\}$ and whether it is completely overlapped by an increment or overlaps adjacent increments in $\{E_n\}$. If $m\Delta$ is the distance in $\{E^t_m\}$ from the start of the set to the end of the m^{th} increment and, beginning with $n = 1$, calculate the difference

$$D_{m,n} = m\Delta - n\Delta' \tag{B2}$$

If $D_{m,n} > 0$, n is incremented by 1 until $D_{m,n} \leq 0$. When this condition is satisfied, the right-hand end of the m^{th} increment in $\{E_m{}^t\}$ lies at or to the left of the right-hand end of the n^{th} increment in $\{E_n\}$. The following difference term is then calculated

$$D_{m-1,n} = (m - 1)\Delta - n\Delta' \tag{B3}$$

If $D_{m-1,n} \geq 0$, then the m^{th} increment in $\{E^t_m\}$ lies within the n^{th} increment in $\{E_n\}$; otherwise it overlaps the n^{th} and $(n - 1)^{th}$ increment. The overlap in the n^{th} increment of $\{E_n\}$ is

$$\begin{aligned} A &= m\Delta - (n - 1)\Delta' = \\ &= [m - (n - 1)](N/N')\Delta \end{aligned} \tag{B4}$$

and in the $(n - 1)^{th}$ increment it is

$$\begin{aligned} B &= (n - 1)\Delta' - (m - 1)\Delta = \\ &= [(n - 1)(N/N') - (m - 1)]\Delta \end{aligned} \tag{B5}$$

When $D_{m-1,n} \geq 0$

$$E^t_m = E_n \tag{B6}$$

otherwise

$$E^t_m = E_n(A/\Delta) + E_{n-1}(B/\Delta) \tag{B7}$$

As a check on the transformation process, the following consistency condition should be satisfied

$$\frac{1}{N'}\sum_{n=1}^{N'} E_n = \frac{1}{N}\sum_{m=1}^{N} E^t_m \tag{B8}$$

This process can be applied to segments of the scanned data. To do this, the equilibrated data set is partitioned into segments that correspond to the same segments (for example, latewood to latewood bands) of equal or different lengths in the unequilibrated data set. The above transformation process is applied to each corresponding segment where the number of data values are denoted as n ($n \leq N$) and n′ ($n' \leq N'$) for the unequilibrated and equilibrated data sets, respectively.

Completion of the transformation process enables the evaluation of the volume ratios V/V′. The sampled volume at each step in the densitometer measurement is determined by the gamma-ray beam cross-section and the thickness of the specimen (Fig. 1). This volume is given by

$$V = \Delta HL \tag{B9}$$

where Δ is the beam width, H is the beam height, and L is the specimen thickness. However, the volume sampled in the equilibrated measurement contains material originally distributed in a larger volume given by

$$V' = \Delta'H'L' \tag{B10}$$

where

$$\Delta' = \Delta(1 + \epsilon) \tag{B11}$$

and

$$H' = H(1 + \gamma) \tag{B12}$$

The correction factors ϵ and γ account for anisotropic shrinkage of specimens. In practice, the scan path across the specimen from face-to-face may not be radial. If θ is the angle between the scan path and the radial direction (Fig. 1), the correction factor γ is

$$\gamma = \left[\frac{\Delta\epsilon\alpha}{H}\right]\left[\frac{\cos\theta + \alpha^{-1}\sin\theta}{\cos\theta + \alpha\sin\theta}\right] \tag{B13}$$

where α is the tangential-to-radial shrinkage ratio.

The required volume ratio is given by

$$\begin{aligned} (V/V') &= (L/L')(1 + \epsilon)(1 + \gamma) = \\ &= (LN'/L'N)(1 + \gamma) \end{aligned} \tag{B14}$$